Proton Delocalization and Hyperacidity in Some Phenolic Resins

Zhenglin Yan, Tung-Feng Yeh,† David G. Schmidling, and Arnost Reiser*

Institute of Imaging Sciences, Polytechnic University, Six Metrotech Center, Brooklyn, New York 11201

Peter A. Mirau

Bell Laboratories, Lucent Technologies, 700 Mountain Avenue, Murray Hill, New Jersey 07974

Libuše Šroubková and Rudolf Zahradník

Heyrovský Institute of the Academy of Sciences, Dolejškova 3, Prague 8, Czech Republic

Received September 11, 2000

ABSTRACT: Interaction between OH groups can produce large acidity increases in phenolic systems. We report here on the behavior of a group of oligomers of *p*-cresol, where the cresol units are linked to each other by $-CH_2-$ bridges. In this series the acid dissociation constant increases consistently with the length of the oligomer chain. The effect is very significant; between the monomeric cresol and the pentamer the acid dissociation constants as measured in organic solvents span 5−8 orders of magnitude. In phenols, part of the acid dissociation energy is the electrostatic work required to separate the incipient ions, and that work depends on the charge located at the oxygen of the corresponding phenolate anion. It appears that with increasing length of the oligomer chain the charge on the anion site decreases. We have found that this is caused by proton delocalization between the oxygen centers of the oligomeric anions. Proton delocalization makes possible the redistribution of charge among all the oxygen centers of the oligomer, thereby lowering the charge on any one of them and increasing the acidity of the monoanions. The reality of proton delocalization is evidenced by the ^{13}C NMR spectra of the monoanions. The two carbon atoms of the dimer anion are indistinguishable and produce a single line in the NMR spectrum and so do the terminal carbons of the trimer anion. These observations are in line with the results of an ab initio calculation indicating an unexpectedly low energy barrier (3.5−0.3 kcal/mol) separating the two equilibrium positions of the proton. It appears that the proton oscillates almost freely between the two positions and is effectively delocalized over both oxygen centers.

Introduction

Novolak resins are among the basic materials of the semiconductor device industry. They are condensation polymers of *p*-cresol and *m*-cresol with formaldehyde, and they come in a variety of (branched) structures and in a range of molecular weights. The following formula is an idealization illustrating the frequent appearance of ortho−ortho-linked phenols in the polymer chain.

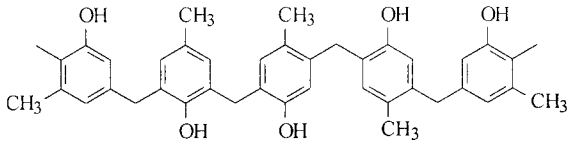

Together with various dissolution inhibitors, Novolaks serve as the common pattern transfer materials (resists) of microlithography.[1,2] They are uniquely suited for this purpose; other phenolic resins produce only low contrast images when used in lithographic applications.[3] Recent work suggested that the cause of this difference in behavior is the high acidity of Novolak.[4] It has been known for some time[5] that Novolak is considerably more acidic than cresol. The source of the hyperacidity of Novolak has become a matter of practical interest since the semiconductor industry had to consider other resins for lithography. That was the original incentive for the present investigation.

† Current address: Polaroid Graphics Imaging, Waltham, MA 02154.

* To whom correspondence should be addressed.

To reduce the Novolak problem to its essentials, we thought of investigating a series of *p*-cresol oligomers where the phenolic units are connected by $-CH_2-$ bridges.[6]

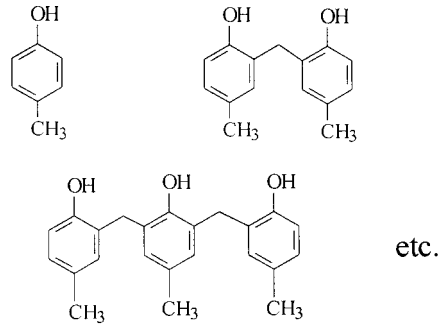

Thomas Sarubbi of Arch Chemicals has kindly provided for us samples of these oligomers up to and including the pentamer. The oligomers are not soluble in water, and we determined their pK_a in a medium of 95% acetonitrile/5% water [7] as well as in pure dimethyl sulfoxide (DMSO). We used a glass electrode following a procedure described by Noyes.[8] It was found that the acidity of the oligomers increased consistently with increasing chain length. In fact, between the monomer (*p*-cresol) and the pentamer, the acid dissociation constants spanned 5 orders of magnitude in DMSO and 8 orders in the mixed solvent. The data are collected in Table 1 and represented in Figure 1.

Others before us were interested in these types of molecules.[9,10] Sprengling[9] for example had titrated a

10.1021/ma0015727 CCC: $20.00
Published on Web 03/24/2001

Table 1. Acid Dissociation Constants (pK_a) of *p*-Cresol Oligomers at 20 °C (a) in 95% Acetonitrile/5% Water and (b) in DMSO

	(a)		(b)	
	pK_a	ΔG(dissoc), kcal/mol	pK_a	ΔG(dissoc), kcal/mol
p-cresol	15.5	21.2	14.9	20.3
dimer	12.5	17.1	13.0	17.7
trimer	10.0	13.6	11.2	15.3
tetramer	7.9	10.8	9.9	13.5
pentamer	7.3	9.96	9.4	12.8

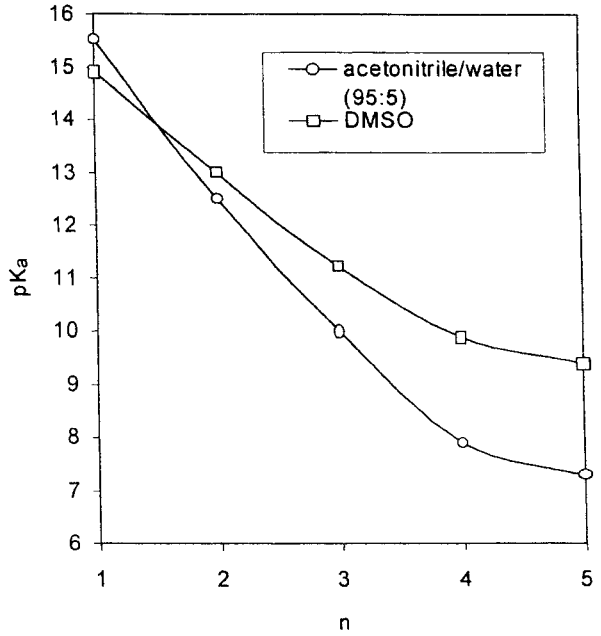

Figure 1. pK_a of the oligomers of *p*-cresol measured in 0.1 M solution in 95% acetonitrile/5% water and in pure DMSO, plotted against the length (*n*) of the oligomer chain.

range of phenolic oligomers in ethylenediamine and later in propanol/benzene mixtures. He found increased acidity in those molecules in which the OH groups were arranged ortho to each other, and he concluded that this "...hyperacidity must be due to the presence of intramolecular hydrogen bonds from one hydroxyl to the other...". It was thought that the high acidity of Novolak is similarly caused by hydrogen bonding,[1,5] the hydrogen bond taking away electron density from oxygen and weakening the covalent OH.

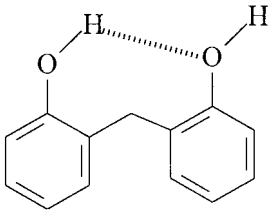

We have now found that in the oligomeric anions hydrogen bonding induces the delocalization of protons between adjacent oxygen centers, leading to the stabilization of the anion and hence to higher acidity.

Before demonstrating this effect on the example of *p*-cresol dimer, we note that the dissociation of phenol into a proton and a phenolate anion goes through a stage where the covalent OH bond is essentially broken, but the two incipient ions are still held together by electrostatic forces.

Table 2. Acidity of Substituted Phenols and Charges on the Oxygen of the Phenolate Anion

		pK_a	
	charge	water	DMSO
1. phenol	0.573	9.84	16.4
2. 4-methyl-	0.568	10.17	
3. 4-chloro-	0.554	9.18	
4. 4-nitro-	0.485	7.15	11.0
5. 2,3-dichloro-	0.525	7.44	
6. 2,4,6-trichloro-	0.493	6.00	
7. 2,4-dinitro-	0.446	3.96	
8. 2,6-dinitro-	0.384		4.9
9. 3,5-dinitro-	0.504		10.6
10. 4-chloro-2,6-dinitro-	0.375		3.5

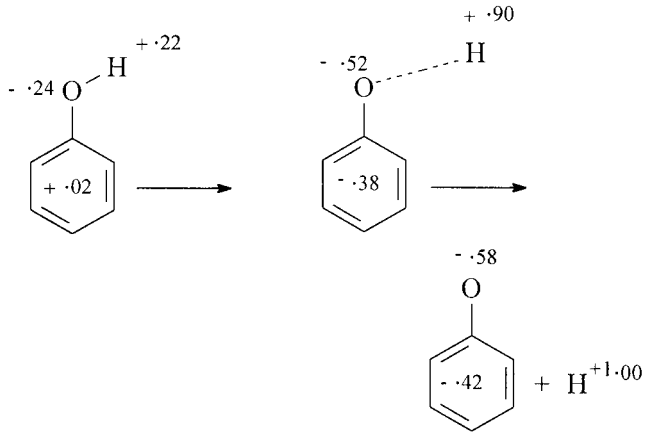

The dissociation energy of phenol has thus an ionic component which is linked to the charge located on the oxygen center of the phenolate anion. The lower that charge, the easier it is for the molecule to dissociate. To illustrate the correlation between pK_a and the charge on the oxygen of the phenolate ion, we have calculated the charges on the oxygen atom for a group of substituted phenolate ions and have confronted them with the pK_a values in water and in DMSO of the corresponding substituted phenols. The data are collected in Table 2 and plotted in Figure 2. The pK_a values in water are those listed in the *Handbook of Chemistry and Physics*, 74th ed. (1993); the pK_a values in DMSO are from a paper by Kolthoff et al.[11] It appears that in both media the pK_a of phenols and the charges on oxygen of the phenolate ions are linearly correlated. We conclude that, to a degree, the acidity of a phenol is linked to the charge on the oxygen of the corresponding phenolate anion. If this is accepted, the data in Table 1 suggest that the charges on the oxygen centers of the oligomer anions decrease with increasing chain length. How such a reduction in charge may come about will be considered in the example of the dissociation of *p*-cresol dimer.

Cyclic Proton Transfer and the Dissociation of the *p*-Cresol Dimer

The first step in the dissociation of the *p*-cresol dimer leads to a monoanion where one of the OH groups is hydrogen bonded to a newly created ionic center. Structure **I** in the partial molecular diagram of Scheme 1 is the result of this transaction. In structure **I** the negative charge on the oxygen of the phenolate ion[12] (0.58 eu) will exert a powerful attraction on the proton of the still intact OH group, and this may lead to a transfer of the proton to the other oxygen center.

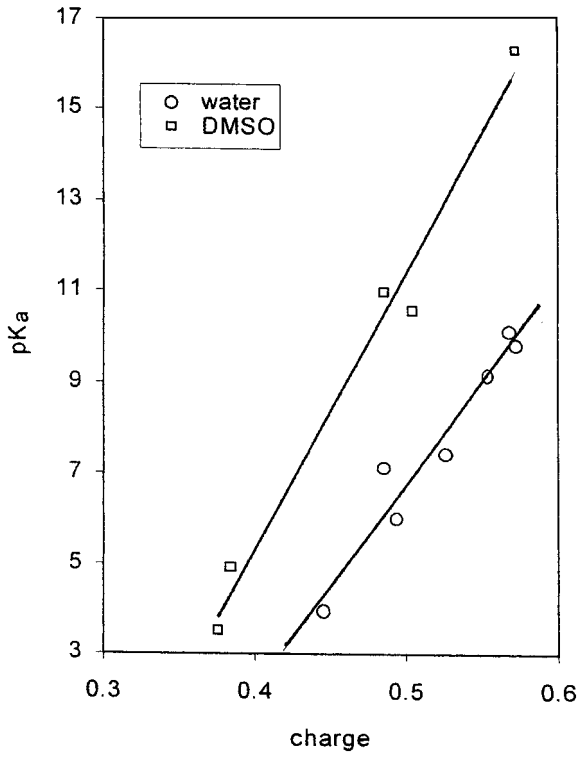

Figure 2. Correlation between the charge on the phenolate oxygen and the pK_a of the corresponding phenols for a group of substituted phenols, measured in water and in DMSO.[10,11]

Structure **I** is thereby transformed into structure **II**. The same process repeats itself, returning the dimer anion to configuration **I**, etc. It is our contention that this process of cyclic intramolecular proton transfer actually occurs. If it does, it will appear to an observer with a time resolution coarser than the interchange frequency that the proton of the dimer is delocalized over both oxygen centers. That observer will not be able to distinguish between the two oxygen centers and will sense a time-average charge [q] on either of them.

$$[q]_{\text{dimer}} = -^1/_2(0.58 + 0.32) = -0.45 \qquad (1)$$

This time-average charge is lower than the charge on the oxygen in the anion of *p*-cresol (which has a value of $[q]_{\text{monomer}} = -0.57$ eu). It appears from this example that cyclic proton transfer provides a mechanism by which the charge on the oxygen centers of the phenolic oligomers is redistributed over all oxygen centers, and the effective (time-average) charge at any one particular center is lowered. Before taking this idea further, we sought experimental support for the reality of cyclic proton transfer in phenolic dimers and trimers.

NMR Spectra of Phenolic Anions

If cyclic proton transfer in the dimer anion occurs at a rate that is faster than the time constant of an NMR measurement, both oxygen centers will appear to be identical, and the ^{13}C NMR spectrum of the dimer anion will show a single peak for the two carbon atoms adjoining the oxygen centers. To test this prediction, we prepared the monolithium salt of the dimer.

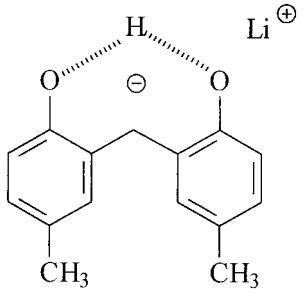

When we measured its carbon-13 spectrum in dilute solution in acetone, we found two peaks for the C−O carbon (Figure 3). That seemed to disprove rapid proton transfer. However, it occurred to us that this result was caused by the strong ionic bond between the small Li^+ ion and one of the oxygen centers. Such a bond would "label" that center and make it different from the other. To lessen the strength of the ionic bond and provide an equal environment for both C−O carbons, we replaced the lithium ion with the much larger tetraethylammonium cation and carried out the measurement in a 1 M solution of tetraethylammonium chloride in DMSO. In that experiment only a single peak for the two C−O carbons was observed (Figure 4). A similar experiment with the anion of the *p*-cresol trimer showed only two C−O carbon signals instead of three (Figure 5). These results indicate that cyclic proton transfer between the oxygen centers of the *p*-cresol dimer and of the *p*-cresol trimer occurs with a frequency at least as high as the time constant of the NMR measurement, which is of the order of 10^3 s^{-1}.

Frequency of Intramolecular Proton Transfer

The NMR measurements described above provide only a lower limit to the frequency of proton transfer in the *p*-cresol dimer anion. A general estimate of this frequency can be derived from the energy barrier separating the two equilibrium positions of the proton. We have estimated this barrier by an ab initio calculation at the Hartree−Fock level and found, in the gas phase, that the energy of the barrier lies only 3.5 kcal/mol above the energy of either equilibrium position. A second aproach using more detailed density functional theory resulted in an even lower value, 0.3 kcal/mol. We believe that the low barrier is caused by a concerted movement of charge in and out of the benzene rings in response to the movement of the proton. The concerted charge shifts lead to a stabilization of the O···H···O moiety in its symmetrical configuration.

When these calculations were repeated in the presence of solvent, the energy barrier was even lower. Geometry and energy parameters for the equilibrium states and for the transition state were used to find a one-dimensional potential function describing the transit of the proton from one equilibrium state to the other. The potential function is in three pieces, smoothly joined, and it incorporates the force constants for the OH stretching mode in equilibrium and in the transition state. The energy is in attojoules (aJ) and distances are in angstroms (Å).

Scheme 1

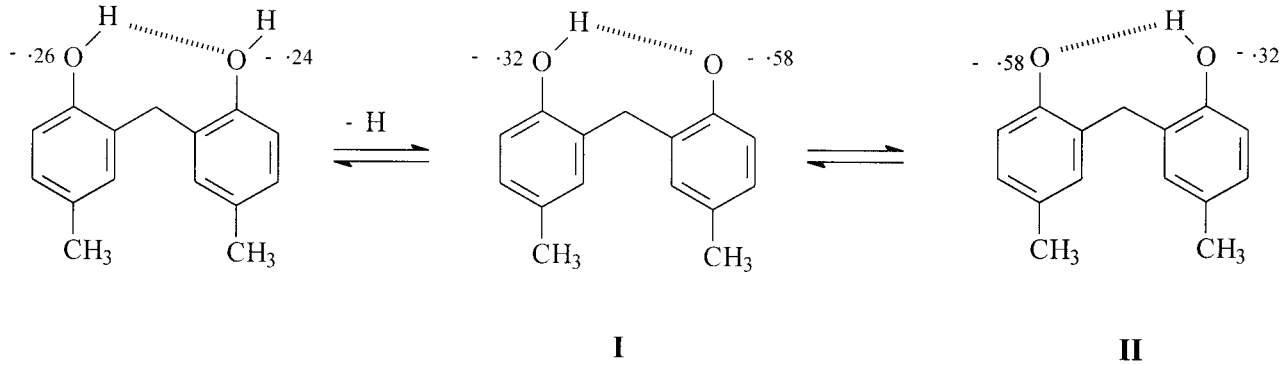

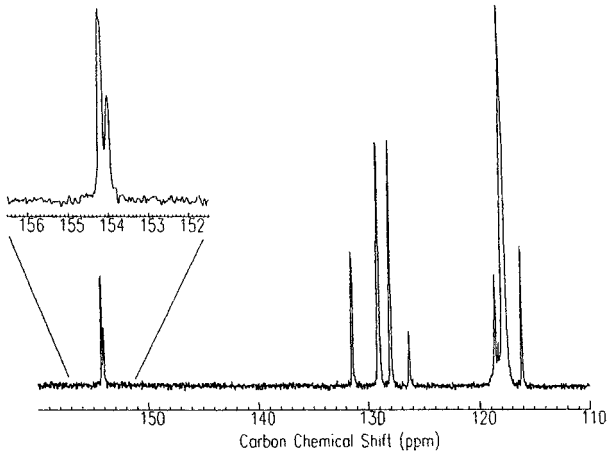

Figure 3. ^{13}C NMR spectrum of monolithium salt of the dimer of *p*-cresol measured in acetone solution. Inset: enlarged trace of signal of the C−O carbons.

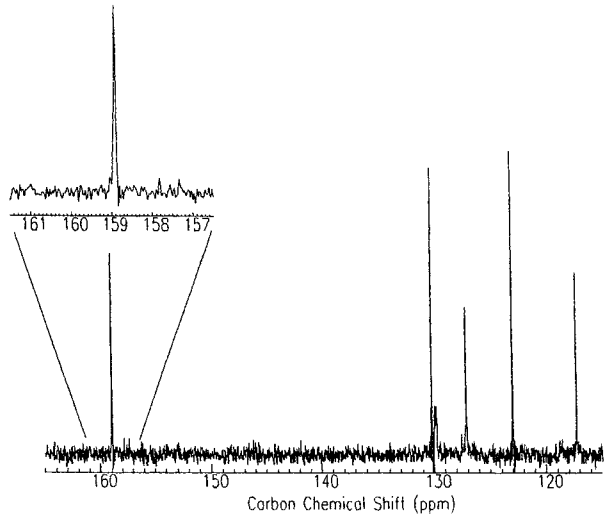

Figure 4. ^{13}C NMR spectrum of monotetraethylammonium salt (0.1 g in 1 mL) of the *p*-cresol dimer dissolved in a 1 M solution of tetraethylammonium chloride in DMSO. Inset: enlarged trace of C−O carbon signals.

$$q < -0.165624 \qquad V = (^1/_2)2.8908(q + 0.1689)^2$$

$$-0.165624 < q < 0.165624 \quad V = 0.002498931 + (^1/_2)(-0.2612)q^2 + 1.85934q^4$$

$$0.165624 < q \qquad V = (^1/_2)2.8908(q - 0.1689)^2$$

The one-dimensional Schroedinger equation was solved using this potential and an effective mass taken to be

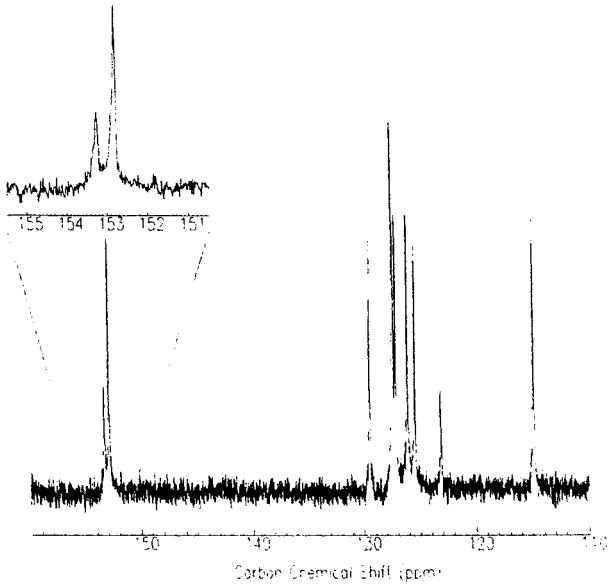

Figure 5. ^{13}C NMR spectrum of the monotetraethylammonium salt of the trimer of *p*-cresol, dissolved in 1 M solution of tetraethylammonium chloride. Inset: enlarged trace of C−O carbon signals.

that associated with the proton in the fictitious vibration in the transition state, 1.1610 amu. The potential energy function and the wave function solutions are presented in Figure 6. Energies associated with these solutions are 1.00, 3.26, 6.72, and 10.59 kcal/mol. The lowest energy level lies below the zero point energy for a single equilibrium configuration alone, as computed in the harmonic approximation. The difference in zero point energies is about 1.7 kcal/mol and represents an additional stabilization of the anion. It should be noted that while the equilibrium positions of the proton are separated by about 0.34 Å, the actual position of the proton is best described as being nearly that of the transition state, even at 0 K. In light of these results, it seems likely that the O···H···O moieties in the higher oligomer anions also have anomalously low zero point energies, and that increases acidity with increasing oligomer size.

The data summarized in Figure 6 support our initial assumption that the proton can transit easily between the two equilibrium positions. The frequency of proton transfer can now be estimated using the Eyring equation.

$$K = \frac{kT}{h} \exp(\Delta G_{\text{transfer}}/RT)$$

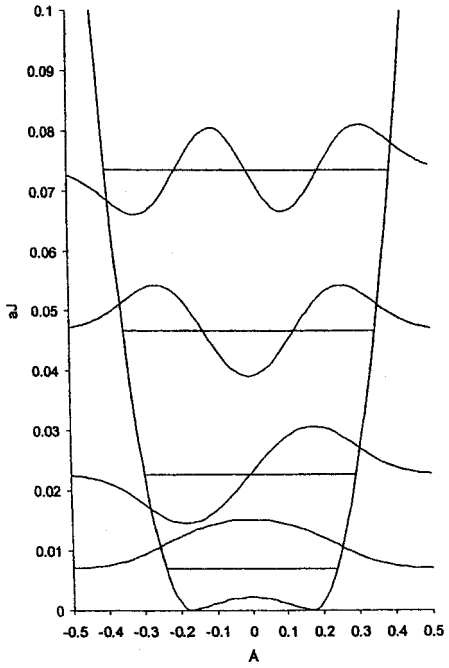

Figure 6. Potential energy function corresponding to the one-dimensional Schroedinger equation for the O···H···O antisymmetric stretching mode in the anion of the *p*-cresol dimer. It is shown here together with the first four energy levels and the corresponding wave functions.

For a free energy barrier of $\Delta G_{transfer} = 5$ kcal/mol (the higher limit of the barrier energy) the proton-transfer frequency at 300 K is $K = 1.5 \times 10^9\ s^{-1}$; for an energy barrier of 1 kcal/mol it is $1.2 \times 10^{12}\ s^{-1}$. Transfer frequencies of this order of magnitude are clearly sufficient to bring about charge averaging with respect to the deprotonation step at the oxygen center of a phenol unit. In the monoanion of the dimer the two potential functions of the phenol units have practically fused into a single energy well: the proton of the dimer anion is effectively delocalized over the whole space between the two oxygen atoms.

Correlation of pK_a with Time-Average Charges on the Oligomer Anions

In the presence of proton delocalization, the first deprotonation step in any *p*-cresol oligomer will result in a single monoanion, irrespective of the site at which the proton originated. For *p*-cresol trimer this unique anion is represented below.

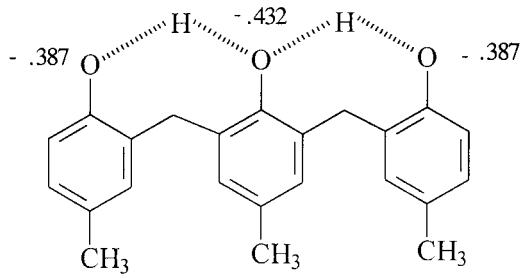

The time-average charges indicated on the molecular diagram are derived from the charges on the oxygen centers in the three static configurations of the trimer ion (i.e., in the absence of proton transfer). Molecular diagrams of these configurations were calculated by the semiempirical Hartree−Fock−Roothaan SCF method[13] using the PM3 parametrization.[13,14] Charge distributions were determined via a Mulliken population analysis.[15] Depending on the location of the anion site, the trimer has three possible static structures, two of which are symmetrically identical. The two nonidentical structures are shown below.

Table 3. Charge Distributions and Average Charges on the "Delocalized" Anions of *p*-Cresol Oligomers

position chain length	1	2	3	4	5	av
1	0.568					0.57
2	0.450	0.450				0.45
3	0.387	0.432	0.387			0.40
4	0.358	0.383	0.383	0.358		0.37
5	0.352	0.370	0.372	0.370	0.352	0.36

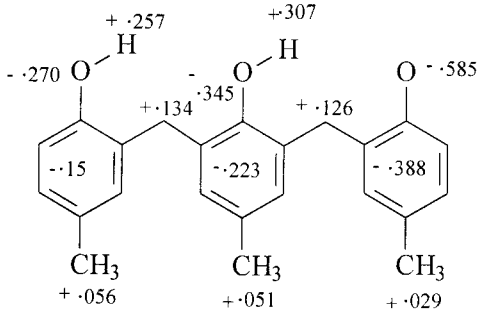

(a) and (c)

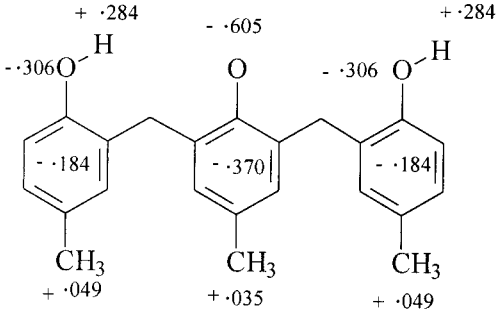

(b)

Time-average charges on the three oxygen centers of the *p*-cresol trimer were approximated as mean values over the three static equilibrium configurations.

Oxygen center:		1	2	3
Configuration	(a)	.270	.345	.584
	(b)	.306	.605	.306
	(c)	.584	.345	.270
Average		-.387	-.432	-.387

Time-average charge distributions on the oxygen centers of the anions of *p*-cresol tetramer and pentamer were determined in a similar way. The data are listed in Table 3.

It is the thesis of this article that the acidity of phenolic oligomers is correlated with the charge on the corresponding phenolate anions. While the charges on the different oxygen centers of the anions are not the same, it is not unreasonable to assume that the oligomer anions may be characterized by the simple mean of the

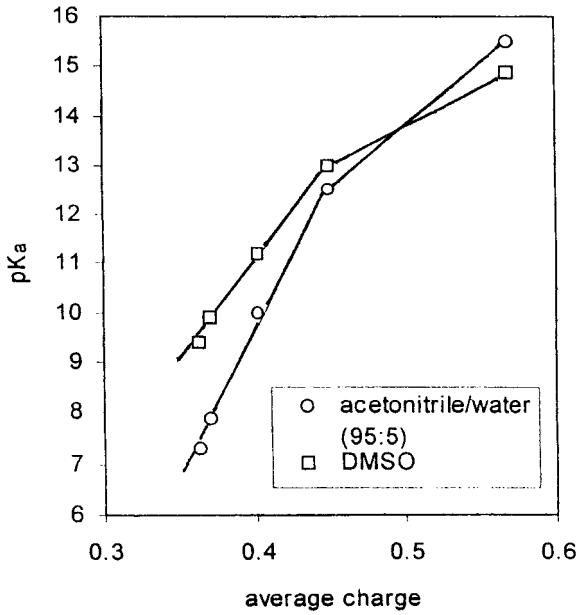

Figure 7. pK_a of the oligomers of *p*-cresol dissolved in 95% acetonitrile/5% water and in DMSO plotted against the calculated overall average charge $\{q\}$ of the monoanions.

time average charges at the individual centers. For the *p*-cresol trimer this overall average charge $\{q\}$ is

$$\{q\} = -^1/_3(0.387 + 0.432 + 0.387) = -0.402 \text{ eu}$$

The overall averages for the anions of the other *p*-cresol oligomers are also listed in Table 3.

To test the connection between anion charge and acidity, we have plotted in Figure 7 the pK_a values of the oligomers against the calculated average charges. The two quantities can be seen to be linearly correlated, with the exception of the data points of the monomer. We note also that the slopes of the correlation lines in Figure 7, namely d(pK_a)/d$\{q\}$, are 42 and 55 for DMSO and for the mixed solvent, respectively. These values are very near the slopes of the correlation lines in Figure 2, which are 62 and 58 for substituted phenols in DMSO and in water. Thus, the relationship between anionic charge and acidity in *p*-cresol oligomers is in line with the behavior of monomeric phenols in similar circumstances.

Conclusion

The initial goal of this study was to discover the source of the hyperacidity of Novolak. While pursuing this goal, we came across an unexpected phenomenon, cyclic proton transfer which effectively delocalizes the proton among neighboring oxygen centers. Proton delocalization brings about a redistribution of charge among the oxygen centers of the anions and lowers thereby the charge on any one of the oxygen centers. The consequence is a lowering of the dissociation energy of the OH groups.

Proton delocalization in phenolic oligomers establishes a communication between the oxygen centers of the molecule. As a result, the charge on any of the phenolate units of an oligomer makes its contribution to the charge level of all other oxygen centers. In these systems proton delocalization has a similar function as electron delocalization has in aromatic molecules where it establishes the communication which finds its expression in the well-known substituent effects.

The hyperacidity of Novolak can now be traced to the interaction between ortho−ortho-linked phenols in the Novolak chain. When two or more phenol units are so linked, charge redistribution occurs among them, and that lowers the dissociation energy of the proton. It is the higher acidity of these blocks which finally increases the acidity of the resin. By comparing the pK_a of a standard Novolak with that of the *p*-cresol oligomers, it appears that on average the ortho−ortho-linked blocks in Novolak are dimers and trimers.

One of the reviewers of this paper has questioned the relevance of our results, obtained in solution, to the behavior of Novolak in a solid matrix. This is a most appropriate observation, and we respond to it with the results of two recent publications. We have been concerned with Novolak dissolution and dissolution inhibition for some time and recently were able to show[18] that the rate of progress of developer base into the matrix depends critically on the concentration of free, dissociated, protons in the films, in other words, on the acid dissociation constant of the phenol groups in solid Novolak. It was that finding that encouraged us to look for the effect of resin acidity on dissolution rate and on inhibitability. It is not practical to measure proton concentrations in the dark matrices of Novolak films, and we have therefore explored the possibility of relating dissolution rate and inhibitability with the acidity of the resin as measured in solution.[19] We found that solid-state inhibitability and solution acidity are indeed correlated not only in Novolak but also in other phenolic resins and that a change in resin acidity will bring about a change in dissolution rate and in inhibitability in the solid resin films. We believe that this makes the present study relevant for the practice of microlithography.

Experimental Section

Materials. Samples of the oligomers were graciously provided by Tom Sarubbi of Arch Chemicals. The oligomers were prepared following the procedures described in ref 6. All other materials were bought from commercial suppliers. Acetonitrile was from J.T. Baker, ACS reagent grade 99%, water was an Aldrich ACS reagent, *p*-cresol, 99% grade, was supplied by Aldrich, and catechol was an Aldrich 99+ reagent.

Determining Acid Dissociation Constants. The pK_a of the oligomers was derived from pH values of known solutions in a mixture of 95% acetonitrile/5% water or in pure, dry DMSO. We used an Accumet 1003 potentiometer from Fischer Scientific, together with an Acumet PH/ATC glass electrode with a double junction Ag/AgCl reference electrode. The experiments were carried out at 20 °C. We followed procedures described by Noyes[8] and by Harlow and Bruss.[17] The measurements were reproducible within ±0.05 units of pH.

To eliminate the effect of phenol/phenol interactions, the pH measurements were carried out at low *p*-cresol or oligomer concentrations. For the measurements in DMSO the concentrations were as follows: 0.0956 M for *p*-cresol, 0.0045 M for the dimer, 0.0032 M for the trimer, 0.0037 M for the tetramer, and 0.0021 M for the pentamer. For the measurements in acetonitrile/water 95:5 the concentration was 0.1 M. In these conditions the pK_a of *p*-cresol and its oligomers was effectively independent of concentration. In both organic solvents the pK_a of the samples was considerably higher than the pK_a of phenol derivatives in water and acidity differences between molecules were amplified.

NMR Measurements. Carbon NMR spectra were recorded on a Varian Unity 400 NMR spectrometer operating at 100 MHz for carbons. The sweep widths were 30 kHz, and the spectra were acquired with 18 μs 90° carbon pulses and proton

decoupling. The samples typically contained 100 mg of oligomer dissolved in 2 mL of solvent, either dry acetone or DMSO.

Calculations. Charge distributions on *p*-cresol and its oligomers were determined using the MOPAC program, versions 6 and 7 (PM3 parametrization). Gas-phase geometries were optimized to a gradient norm of 0.05 kcal/mol or less. Solvent effects were estimated by the COSMO method again based on a PM3 parametrization. Two effects were noted: the changes in deprotonation energy were smaller in the solvent than in the gas phase, and second, the differences in the deprotonation energies of the OH groups in different positions were smaller than in the gas phase.

Before calculating the molecular data, we considered several possible steric conformations of the oligomer chains. Local energy minima for the oligomers are characterized by methylene−phenyl torsion angles of roughly ±90° relative to a planar structure. A conrotatory (+ +) pair of torsions leads to a structure with approximetly C_2 local symmetry and an O−O distance of about 5.5 Å in which hydrogen bonding is essentially absent. A disrotatory pair of torsions leads to a structure of approximately C_s symmetry with an O−O distance of about 2.7 Å where hydrogen bonding is present. In all the oligomers with more than one methylene group every combination of positive and negative torsions yields a local minimum. The gas phase global energy minima have local CS symmetry at each methylene, with the torsions in a pattern (+ −, − +, + −, ...) featuring an extended pleated structure and an extended chain of hydrogen bonds. The calculated charges are quoted for this slightly puckered quasi-planar conformation. The time-average charge distributions for the anions were obtained as averages at the individual oxygen centers.

The ab initio calculations on the dimer anion at the Hartree−Fock level used a 6-31G(d) basis set. The calculation using density functional theory (B3LYP) was performed on the basis set 6-311++G(3df, 3dp). Both calculations used the Gaussian program.[14]

Acknowledgment. The work reported here has been largely supported by a grant from the Semiconductor Research Corporation. It has also been supported by smaller grants from the Xerox Corporation, from DuPont, and from St. Jean Photo-Chemicals. We acknowledge with great pleasure valuable conversations with Mark Green and with Herbert Morawetz, both of Polytechnic University.

References and Notes

(1) Dammel, R. *Diazonaphthoquinone-based Resists;* SPIE Tutorial Text 11; SPIE Press: Bellingham, WA, 1993; Chapter 2.
(2) Reiser, A.; Shih, H.-Y.; Yeh, T.-F.; Huang, J. P. *Angew. Chem., Int. Ed. Engl.* **1996**, *35*, 2429.
(3) Willson, C. G. In *Introduction to Microlithography*, 2nd ed.; Thompson, L. F., Willson, C. G., Bowden, M. J., Eds.; American Chemical Society: Washington, DC, 1994; Chapter 3.
(4) Flanagin, L. W.; McAdams, C. L.; Hinsberg, W. D.; Sanchez, I. C.; Willson, C. G. *Macromolecules* **1999**, *32*, 5337.
(5) DeRosa, T. F.; Pearce, E. M.; Charton, M. *Macromolecules* **1985**, *18*, 2277, 2282.
(6) Jeffries, A. T., III.; Honda, K.; Blakeney, A. J.; Tadros, S. US Patent No. 5,196,289 of March 23, 1993.
(7) Yan, Zh.; Reiser, A. *Macromolecules* **1998**, *31*, 7723.
(8) Noyes, R. M. *J. Am. Chem. Soc.* **1962**, *84*, 513; **1964**, *86*, 971.
(9) Sprengling, G. R. *J. Am. Chem. Soc.* **1954**, *76*, 1190.
(10) Chatterjee, S. K. *Can. J. Chem.* **1969**, *47*, 2323.
(11) Kolthoff, I. M.; Chantooni, M. K.; Bhowmik, S. *J. Am. Chem. Soc.* **1968**, *90*, 25.
(12) The charges indicated above were obtained by PM3 calculations for the species in the gas phase. They would be slightly different in the solvent. These differences, however, do not affect our argument.
(13) Stewart, J. P. *J. Comput. Chem.* **1989**, *10*, 209, 221.
(14) Gaussian 94: Frisch, M. J.; Pople, J. A.; et al.; Gaussian Inc., Pittsburgh, PA, 1995.
(15) Mulliken, R. S. *J. Chem. Phys.* **1955**, *23*, 1833.
(16) Klamt, A.; Schuurmann, G. *J. Chem. Soc., Perkins Trans. 2* **1993**, 799.
(17) Harlow, G. A.; Bruss, D. B. *Anal. Chem.* **1958**, *30*, 1833.
(18) Reiser, A.; Yan Zh.; Han Y. K.; Kim, M. S. *J. Vac. Sci. Technol* **2000**, *B18*, 1288.
(19) Yan, Zh.; Yeh, T.-F.; He, X.; Reiser, A.; Schadt, F. L. III.; Fincher, C. R. *J. Vac. Sci. Technol.* **2000**, *B18*, 2745.

MA0015727